



Aalborg Universitet

AALBORG UNIVERSITY  
DENMARK

## Wireless Control of Modular Multilevel Converter Submodules With Communication Errors

Ciftci, Baris; Harnefors, Lennart; Wang, Xiongfei; Gross, James; Norrga, Staffan; Nee, Hans Peter

*Published in:*  
IEEE Transactions on Industrial Electronics

*DOI (link to publication from Publisher):*  
[10.1109/TIE.2021.3125664](https://doi.org/10.1109/TIE.2021.3125664)

*Creative Commons License*  
CC BY 4.0

*Publication date:*  
2022

*Document Version*  
Publisher's PDF, also known as Version of record

[Link to publication from Aalborg University](#)

*Citation for published version (APA):*  
Ciftci, B., Harnefors, L., Wang, X., Gross, J., Norrga, S., & Nee, H. P. (2022). Wireless Control of Modular Multilevel Converter Submodules With Communication Errors. *IEEE Transactions on Industrial Electronics*, 69(11), 11644-11653. <https://doi.org/10.1109/TIE.2021.3125664>

### General rights







Copyright and moral rights for the publications made accessible in the public portal are retained by the authors and/or other copyright owners and it is a condition of accessing publications that users recognise and abide by the legal requirements associated with these rights.

- Users may download and print one copy of any publication from the public portal for the purpose of private study or research.
- You may not further distribute the material or use it for any profit-making activity or commercial gain
- You may freely distribute the URL identifying the publication in the public portal -

### Take down policy

If you believe that this document breaches copyright please contact us at [vbn@aub.aau.dk](mailto:vbn@aub.aau.dk) providing details, and we will remove access to the work immediately and investigate your claim.

# Wireless Control of Modular Multilevel Converter Submodules With Communication Errors

Bariş Çiftçi , *Student Member, IEEE*, Lennart Harnefors , *Fellow, IEEE*,  
Xiongfei Wang , *Senior Member, IEEE*, James Gross , *Senior Member, IEEE*,  
Staffan Norrga , *Member, IEEE*, and Hans-Peter Nee , *Fellow, IEEE*

**Abstract**—Wireless control of modular multilevel converter (MMC) submodules can benefit from different points of view, such as lower converter cost and shorter installation time. In return for the advantages, the stochastic performance of wireless communication networks necessitates an advanced converter control system immune to the losses and delays of the wirelessly transmitted data. This article proposes an advancement to the distributed control of MMCs to be utilized in wireless submodule control. Using the proposed method, the operation of the MMC continues smoothly and uninterruptedly during wireless communication errors. The previously proposed submodule wireless control concept relies on implementing the modulation and individual submodule-capacitor-voltage control in the submodules using the insertion indices transmitted from a central controller. This article takes the concept as a basis and introduces to synthesize the indices autonomously in the submodules during the communication errors. This new approach allows the MMC continue its operation when one, some, or all submodules suffer from communication errors for a limited time. The proposal is validated experimentally on a laboratory-scale MMC.

**Index Terms**—Autonomous control, modular multilevel converter (MMC), prototype, resonant controller, wireless control.

## I. INTRODUCTION

MODULAR multilevel converters (MMCs) are widely used in high-voltage dc (HVdc) transmission applications as they can be scaled up easily to high voltage and power ratings using off-the-shelf power semiconductors. The total number of MMC submodules required to reach the targeted ratings might be in the range of a few thousand [1]. The submodules are communicated originally with direct optical fiber cables to the central/master controller(s) [2]. The implementation and operation of optical fiber cables might be quite challenging as

the ratings and size of the MMC increase. The dimensions of the MMC valve halls used in HVdc applications might range hundreds of meters [3]. Consequently, the total length of fiber cables to lay out in the hall goes up to tens of kilometers. Laying out, terminating, and insulation testing this much of and long cables require significant workforce and time during the installation of the MMC. Each cable needs to be identified and checked whether it originates and terminates at the correct terminals during the commissioning, further increasing the required resources [4]. The cable bundles can be cumbersome to route and require resource-intensive mechanical design procedures. The cables lead to an increase in the station footprint as well as the weight and size of the MMC, which are issues especially in offshore transmission platforms [5]. The bundles might also complicate removing and replacing a failed submodule or other components during maintenance, leading to a long maintenance time. Furthermore, the cables create an insulation breakdown risk between the controller and the submodules due to, e.g., the accumulation of dust and humidity on them. Another risk factor for the fiber cables is a fire in the MMC hall. Although the cables do not ignite themselves, they might burn and spread the fire in the hall [6].

Distributed control methods with, e.g., ring or common bus communication networks between the controller(s) and submodules have been proposed as a (partial) solution to the abovementioned challenges, as well as to share the processing workload among different controllers [7]–[11]. The increase of communication latency with the number of submodules connected to the same ring or bus and the limitation of redundancy and online reconfiguration capability in case of failures are the challenges in these applications introduced by eliminating direct communication links. Wireless control of MMC submodules is proposed in [12] and implemented and verified in [13] as a solution alternative for all the previous challenges. By eliminating the optical fiber cables at all, the required workforce and time during the installation, commissioning, and maintenance of the MMC are significantly reduced. The communication latency is independent of the number of submodules in the proposed wireless control method. Moreover, a direct link between the controller(s) and the submodules can be sustained with wireless communication. Although wireless communication brings its own challenges [13], some of which will be mentioned in the next paragraph and another is setting up a wireless network in the MMC hall, the alternative should not be overlooked since the

Manuscript received May 5, 2021; revised September 10, 2021; accepted October 26, 2021. Date of publication November 11, 2021; date of current version June 6, 2022. (Corresponding author: Baris Ciftci.)

Bariş Çiftçi, Xiongfei Wang, James Gross, Staffan Norrga, and Hans-Peter Nee are with the KTH Royal Institute of Technology, SE-10044 Stockholm, Sweden (e-mail: bacif@kth.se; xwa@et.aau.dk; james.gross@ee.kth.se; norrga@kth.se; hans@kth.se).

Lennart Harnefors is with the ABB Corporate Research, 72178 Västerås, Sweden (e-mail: lennart.harnefors@se.abb.com).

Color versions of one or more figures in this article are available at <https://doi.org/10.1109/TIE.2021.3125664>.

Digital Object Identifier 10.1109/TIE.2021.3125664

challenges might be overcome by using advanced controllers as in this article and an adequately engineered wireless network.

The stochasticity of wireless communication, which generally results in higher latency and lower reliability than wired communication, is a major challenge before achieving adequate control of the MMC submodules. Wireless communication with low latency and high reliability for time-critical processes can be considered as a solution [14], [15]. However, low latency and high reliability generally contradict each other in wireless communication, and some degree of errors are inevitable. Thus, a wireless submodule control system should withstand higher latency and lower reliability of the wirelessly transmitted data. The wireless control implemented in [13] is based on broadcasting the insertion indices of phase arms from a central controller and performing the modulation in the submodule controllers. The randomness in the transmission latency is minimized by providing a concordant converter control method and a wireless communication network. The packet losses (communication errors) are resolved by decreasing the closed-loop current control bandwidth and using the last received index for modulation during the packet loss interval. Although this treatment works fine for the losses in the range of a few transmission cycles, the submodules are unprotected for longer losses from tens to hundreds of transmission cycles. The MMC should be prepared for those as they can lead to overcurrents on the ac- and dc-sides and overvoltages in the submodule capacitors [13]. Moreover, the modulation is not sinusoidal when the last received insertion index is used in the packet loss intervals, which causes degradation in the ac-side voltage quality and submodule capacitor voltage balance. The degradation would increase as more submodules suffer losses at the same time.

Fail-safe operation methods against communication failures in MMCs with wired communication networks have been researched previously. Measures against a submodule or one communication link failure in MMCs with ring network are given in [8] and [16]. A resilient operation method is proposed during the packet loss interval for MMCs with distributed control architecture in [17]. The proposed method relies on forming the insertion indices of the affected submodules in their own controllers based on the last fundamental period ac-side voltage or current phase angles before the loss instant. The method works effectively for submodules operating in the steady state but can be less efficient if there is a change in the phase angles in the last fundamental period. Moreover, it is assumed that all the submodules operate at the rated operating point before the packet losses, which is likely for MMCs in HVdc transmission applications but cannot always be assured.

This article takes the wireless control method of [13] as the basis. In order to improve the treatment of packet losses, a submodule is proposed to continue the modulation during the packet loss interval with the same pattern as before the wireless packet loss occurred. For this aim, the insertion index is generated autonomously in the submodule during the loss interval. The generated indices are based on the previously received ones. A set of resonant controllers and a moving average filter (MAF) are employed for this purpose. Resonant controllers [18] have been offered extensively in various power electronics

applications [19]–[22]. They are employed to extract the ac harmonics of the converter current reference in [19] and used in current control schemes while tuned to different reference ac harmonics in [20] and [22]. A comprehensive analysis and applications of resonant controllers are presented in [21]. This article employs the resonant controllers and an MAF to generate the ac and dc components of the insertion indices, respectively, in a submodule. The submodule uses the sum of those for modulation during the packet loss interval. The submodule resumes using the received indices as soon as the wireless communication is recovered. The contribution of this article can be summarized as follows:

- 1) The modulator in the packet-loss-affected submodule(s) (can be one, some, or all) obtains an updated insertion index in the packet loss intervals, and the submodule(s) can continue sinusoidal modulation smoothly as if no packet loss occurred.
- 2) The proposed method can adapt to the changes in the received insertion indices in the last fundamental period before the packet loss. Also, it is independent of the operating point of the submodules.

The structure of the article is as follows. In Section II, the wireless control of MMC submodules is reviewed. In Section III, the proposed autonomous submodule controller is presented and analyzed. Section IV contains the implementation of the proposal on a laboratory-scale MMC and the experimental results. Section V concludes the article.

## II. WIRELESS CONTROL OF MMC SUBMODULES

### A. Existing Wireless Control of MMC Submodules

The autonomous submodule control, which is explained in the next section, is based on the wireless control method of MMC submodules given in [13]. This section is a summary of MMC control in general and its implementation for wireless submodule control. The reader is referred to [13] for the details.

The wireless control of submodules relies on the distributed control approach, which has been investigated by several researchers using wired communication methods [7]–[11]. In the distributed control of MMCs, there is a central controller at the top of the control hierarchy, and local controllers are in the submodules. The central controller and the submodule controllers share the control and measurement data via a communication network. The central controller receives the ac-side (output) current reference from a power-system-level controller and performs ac-side current control, circulating current control, and arm-balancing control. The submodule controllers perform the individual submodule-capacitor-voltage control and modulation.

The control block diagram of the MMC in [13] for the central controller and one submodule controller in an arbitrary-phase upper arm is shown in Fig. 1(a). In the figure,  $i_s^*$  and  $i_s$  are the reference and measured ac-side currents,  $v_a^f$  is the feedforward ac-bus (point of common coupling) voltage,  $v_s^*$  is the ac-side voltage reference,  $i_c^*$  and  $i_c$  are the reference and measured circulating currents,  $v_{cu}^\Sigma$  is the sum capacitor voltage of the arm,  $n_u$  is the arm insertion index, and  $v_{cu}^i$ ,  $n^i$ , and  $s^i$  are the

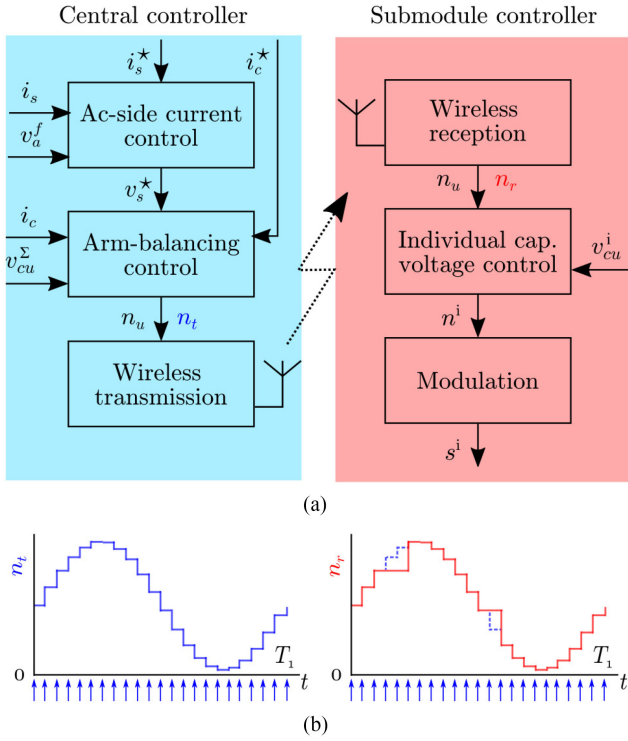


Fig. 1. (a) Overall block diagram of the central and submodule controllers for the MMC submodules existing wireless control. (b) Illustration of the transmitted and received insertion indices. The arrows below the indices correspond to the sampling instants.

capacitor voltage, the insertion index, and the switching signal of the submodule  $i$ , respectively. The central and all the submodule controllers have wireless communication capability. After the ac-side current control in the central controller, open-loop arm-balancing control is preferred [23]. The primary control data transmitted from the central controller to the submodule controllers are the insertion indices of the submodules, which are updated in the range of tens to hundreds of microseconds. The insertion indices of all the phase arms form a single wireless data packet after each sampling period. The packet is broadcast from the central controller immediately after its forming. The physical layer of the IEEE 802.11a protocol with 5825 MHz transmission center frequency is used for wireless communication. Following the reception of the packet, each submodule picks the index corresponding to the phase arm that it belongs to and tunes the index for its own submodule-capacitor-voltage control. Then, the modulation is carried out by phase-shifted carrier-based modulation. The phase-shifted carriers are synchronized periodically in the submodules. The broadcast data packets contain the insertion indices of the six arms, arm currents, dc-side voltage, synchronization flag for carriers, and other auxiliary data. The arm currents and ac-bus voltages are fed back to the central controller with wired communication.

### B. Wireless Communication Issues

Steady-state operation of MMCs generates interference in the sub-GHz frequency range in the converter hall [24], [25] and does not present a threat for communication in the GHz range, as in [13]. However, high-power transients resulting from,

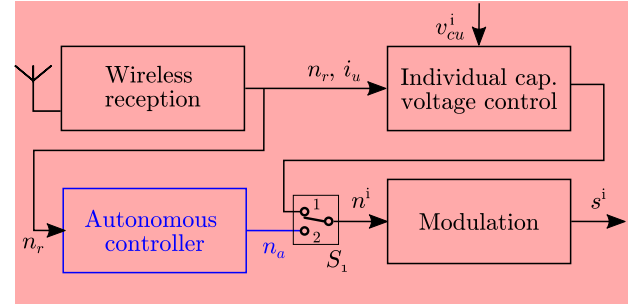


Fig. 2. Proposed submodule controller block diagram.  $S_1$  switches to position 2 when packet loss is decided.

e.g., electrical arcs and circuit breaker operations can interfere with communication [26], [27]. Moreover, noise, deep fading, co-/adjacent channel interference, and even cyber-attacks can influence wireless communication [28]–[30]. As a result, in the wireless control of MMC submodules, wireless data reception may be interrupted for a single or multiple transmission cycles in one, some, or all of the submodules. The losses can be highly time-varying and can have bursty characteristics [31]. They are also dependent on the employed radio parameters. In these circumstances, the transmitted and received insertion indices,  $n_t$  and  $n_r$ , are illustrated below the central controller and the submodule controller in Fig 1(b), excluding the communication delay.  $n_r$  contains random packet losses with variable lengths.

## III. AUTONOMOUS SUBMODULE CONTROL

The proposed approach to deal with the wireless packet losses is to render the submodules generate their insertion indices locally during the interval that they do not receive data from the central controller. The previously received indices can be exploited for this purpose. Fig. 2 shows the proposed block diagram of the submodule controller compared to the one in Fig. 1.  $n_a$  is the autonomously generated insertion index and  $i_u$  is the upper arm current. During normal operations, i.e., when wireless data packets are received, the autonomous controller block is bypassed by the switch  $S_1$ , as shown in the figure, and the index from the central controller,  $n_r$ , is used in the individual capacitor-voltage control and modulation. When the submodule controller takes the *packet loss* decision,  $S_1$  switches to position 2, and  $n_a$  is used in the modulation. The received insertion indices feed the autonomous controller, and it is ready to be in effect in the modulation any time as soon as the packet loss decision is taken. In the following sections, the detection of packet losses and the autonomous controller design are detailed.

### A. Detection of Packet Loss

The first task of autonomous submodule control is to realize if the wireless packets are being received properly or not. With the wireless control method described in Section II, the submodules should ideally receive a new insertion index with a period equal to the MMC sampling period,  $T_s$ . Then, the packet loss can be detected in the submodule controllers using a timer with a predefined threshold. Each packet reception resets the timer. If the timer value exceeds the threshold, the controller concludes



with a packet loss and switches into the autonomous control mode. The controller is back to the normal operation mode when a wireless packet is received again. The threshold,  $T_{\text{loss}}$ , can be defined as

$$T_{\text{loss}} = (1 + r)T_s \quad (1)$$

where  $r$  is a real number between 0 and 1 and corresponds to any possible variance in the packet reception period.  $r$  can be chosen close to 0 if the variance is minimized; however, it is still a random variable in practice.  $T_{\text{loss}}$  in (1) is the minimum realizable value, but not the optimum one. Having  $T_{\text{loss}}$  as in (1) results in unnecessary control mode transitions during the normal packet reception intervals for any two consecutive receptions in which the latter is received with a slightly higher  $r$  value than the one fixed in (1). Even though frequent control mode transitions do not necessarily result in a problem, they are not desirable for a control system.

The closed-loop current control bandwidth in [13] is defined as

$$\alpha_c \leq \frac{\omega_s}{10(k+1)} \quad (2)$$

where  $\omega_s$  is the angular sampling frequency and  $k$  is a non-negative integer. Then, the MMC is robust against at most  $k$  consecutive packet losses without losing stability. If  $\alpha_c$  is decreased anyhow (e.g., to provide a stable closed-loop control or a smoother dynamic response), then the threshold can be prolonged as

$$T_{\text{loss}} = (1 + r + k)T_s. \quad (3)$$

It is important to note that, even if it is possible to prolong  $T_{\text{loss}}$  from the stability point of view as in (3), in the event of packet losses, it is better to switch to the autonomous mode as soon as possible. In this way, the use of same insertion index for modulation, which degrades the ac-side voltage harmonic quality and submodule capacitors voltage balance, is minimized. Thus,  $T_{\text{loss}}$  is advised to be  $(2 + r)T_s$ , unless  $k$  is 0. Consequently, when the wireless communication is malfunctioning, the submodules operate with the same insertion index for at most two sampling periods (excluding  $r$ ), which are short enough to cause no voltage harmonic quality issue or capacitor-voltage unbalance in almost any operational condition.

### B. Design of Autonomous Submodule Controllers

The central controller block diagram was shown in Fig. 1. The primary wireless data, i.e., the insertion indices, are generated in the central controller as

$$n_u = \frac{v_c^* - v_s^*}{v_{\text{cu}}^{\Sigma}} \quad n_l = \frac{v_c^* + v_s^*}{v_{\text{cl}}^{\Sigma}}, \quad (4)$$

where  $v_c^*$  is the internal voltage reference [32].  $v_c^*$  and  $v_s^*$  are produced by the circulating-current controller (included in the arm-balancing control block in Fig. 1) and the ac-side-current controller, respectively. Proportional-resonant (PR) controllers in the stationary reference frame in single-phase or three-phase MMCs can be used for these controllers.

The transfer function of  $v_s^*$  using a PR controller in the ac-side current control block is given by

$$v_s^* = \left( K_p + \frac{K_1 s}{s^2 + \omega_1^2} \right) e + v_a^f \quad e = i_s^* - i_s \quad (5)$$

where  $s$  is the Laplace variable,  $K_p$  is the proportional gain,  $K_1$  is the resonant gain, and  $\omega_1$  is the fundamental angular frequency. Assuming that  $i_s^*$  comprises only the fundamental frequency ac component,  $v_s^*$  contains a dominant fundamental frequency component. Due to the proportional gain, harmonic components (baseband harmonics or switching harmonics) in the measured ac-side current are fed back, and therefore,  $v_s^*$  also contains ac components with these frequencies. In three-phase converters,  $v_s^*$  can also contain a third harmonic voltage component to extend the linear region of the modulation index beyond 1.

The circulating current controller mainly tries to suppress the second harmonic, which emanates from the total-energy ripple of the submodule capacitors of a phase leg. The transfer function of  $v_c^*$  using a PR controller is given by

$$v_c^* = \frac{V_{\text{dc}}}{2} - Ri_c^* - R_a \left[ 1 + \frac{K_r s}{s^2 + (2\omega_1)^2} \right] (i_c^* - i_c) \quad (6)$$

where  $V_{\text{dc}}$  is the dc-side voltage,  $R$  is arm parasitic resistance,  $R_a$  is an active (virtual) resistance,  $K_r$  is the resonant gain, and  $i_c^*$  is the reference (typically dc) circulating current. Apart from the second harmonic component, the controller may have additional resonant controllers tuned to fourth, sixth, and higher order even harmonic components. In such cases,  $v_c^*$  also contains the reference voltage components corresponding to those. Consequently,  $v_c^*$  comprises a dc component, a second harmonic component, and potentially other even harmonics.

The sum capacitor voltages  $v_{\text{cu}/1}^{\Sigma}$  are either assumed constant and equal to  $V_{\text{dc}}$ , measured, or estimated from  $v_c^*$  and  $v_s^*$ . If measured or estimated (as in this article by the method in [23]), they contain at least the fundamental and the second harmonic components apart from the dominant dc-side voltage.

Considering the analyses of  $v_s^*$ ,  $v_c^*$ , and  $v_{\text{cu}/1}^{\Sigma}$ , the ideal insertion indices are linear combinations of these three quantities independent of whether the control is wired or wireless. The indices consist of a dc component, the fundamental frequency ac component, and harmonics of the fundamental. This decomposition forms a valuable basis for the autonomy of the submodules. In the submodules, the dc component of the received insertion indices can be derived by an MAF and the ac components by a set of resonant controllers. In the event of a packet loss, recomposing these components in the submodule controller with the correct magnitude and phase underlies the autonomous generation of insertion indices in the submodules.

The proposed block diagram of the autonomous controller is shown in Fig. 3, and it is included in the submodule controller, as shown previously in Fig. 2. The received  $n_r$  is forwarded into the autonomous controller, but its output  $n_a$  is used in the modulation block only when a packet loss decision is taken.  $n_a^{\text{ac}}$  and  $n_a^{\text{dc}}$  represent the ac and dc components of  $n_a$ , respectively. The switches  $S_2$  and  $S_3$  in Fig. 3 switch to position 2 when a packet loss is decided, as so does  $S_1$  in Fig. 2 simultaneously.

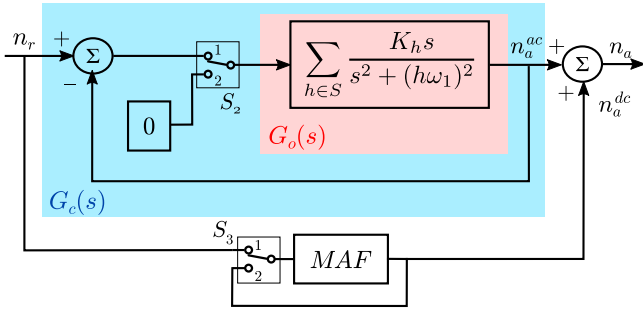


Fig. 3. Autonomous controller block diagram. The switches  $S_2$  and  $S_3$  switch to position 2 when packet loss is decided.

The components of the autonomous controller and the details on their operation are given in the following sections.

**1) Resonant Controllers:** The open-loop transfer function of the set of resonant controllers in the submodules is

$$G_o(s) = \sum_{h \in S} \frac{K_h s}{s^2 + (h\omega_1)^2} \quad (7)$$

where  $K_h$  is the gain,  $h$  is the harmonic number,  $\omega_1$  is the fundamental angular frequency, and  $S$  is the set of harmonic components comprising the insertion indices. The closed-loop transfer function of the set of resonant controllers with negative feedback is

$$G_c(s) = \sum_{h \in S} \frac{K_h s}{s^2 + K_h s + (h\omega_1)^2}. \quad (8)$$

While the open-loop system is marginally stable, the closed-loop system is asymptotically stable with any positive  $K_h$ . The  $G_c(s)$  components have a resonant peak with gain 1 centered at  $s = jh\omega_1$ . The width of the peaks is dependent on the respective gain  $K_h$ . As  $K_h$  increases, the resonant peak gets wider, the controller becomes less selective to the frequency variations, and it has a faster transient response. The suitable value of  $K_h$  can be set according to the desired transient response and frequency selectivity of the controller. During the packet-loss-free operation, i.e.,  $S_2$  is in position 1, for an input signal that is a linear combination of ac harmonics as in  $n_{u/l}$ , the harmonics with the frequency  $h\omega_1$  pass through  $G_c(s)$  with no change in the amplitude and phase, while the other components are damped out. When the communication is lost, the feedback loop is broken by switching  $S_2$  to position 2. In this case, the resonant controller is back to its marginally stable state  $G_o(s)$ . Note that, at the moment  $G_c(s)$  is back to  $G_o(s)$ , the input to the set of resonant controllers also shifts from a nonzero value to zero, which is a Dirac delta function. The controllers then act as an oscillator keeping the amplitude and phase of their outputs, which together comprise  $n_a^{ac}$ , before breaking the feedback loop. Practically, this corresponds to the generation of the ac components of the insertion index.

**2) Moving Average Filter:** An MAF with input signal  $x(t)$  and output signal  $\bar{x}(t)$  is described in the continuous-time domain by

$$\bar{x}(t) = \frac{1}{T_w} \int_{t-T_w}^t x(\tau) d\tau \quad (9)$$

where  $T_w$  is referred to as window length [33]. The MAF frequency response can be obtained as

$$G_{\text{MAF}}(j\omega) = \left| \frac{\sin(\omega T_w/2)}{\omega T_w/2} \right| \angle -\omega T_w/2. \quad (10)$$

The MAF passes the dc component of  $x(t)$  and blocks the ac components, which are integer multiples of  $1/T_w$  in hertz. Thus, to derive the dc component of the insertion indices,  $T_w$  should be chosen as  $1/f_1$ , where  $f_1$  is the fundamental frequency of the ac-side voltage.

In the submodule controllers, the MAF needs to be implemented in discrete-time as

$$\bar{n}_{u/l}(k) = \frac{1}{N} \sum_{i=0}^{N-1} n_{u/l}(k-i) \quad (11)$$

where  $N$  is the filter length and is equal to  $1/f_1 T_s$ . The MAF output  $\bar{n}_{u/l}(k)$  (denoted as  $n_a^{dc}$  in Fig. 3) has  $(N-1)/2$  samples delay, and this might seem like a threat to the stability of the closed-loop control at first glance. However, the autonomous controller, thus the MAF, is bypassed during the normal operation, and the related delay is not included in the closed-loop control system of the MMC. When a packet loss is detected, to avoid  $n_a^{dc}$  converging to the last received  $n_r$ ,  $n_a^{dc}$  is fed back to MAF input by switching  $S_3$  to position 2.

### C. Discussion on the Autonomous Control

The packet losses are a natural phenomenon in wireless communication, and the proposed autonomous control can work effectively for short but the most frequent wireless packet losses. As the loss length increases, the occurrence decreases [31]. If the MMC is in steady-state conditions, the control of submodules with the generated indices will continue finely with longer packet losses too. However, two phenomena can distort the steady-state conditions during the autonomous control and make the generated indices obsolete as the loss gets longer. The first phenomenon is related to the fact that the control with the generated indices is not a closed loop. If there is any change in the circuit parameters or active/reactive power references during the autonomous control interval, the submodules in the autonomous control mode would not respond as desired. A disturbance in, e.g., the dc-side or point of common coupling voltages during the autonomous control would lead to off-reference circulating and ac-side currents (which might be above the component ratings in extreme cases) until the communication is recovered. The second phenomenon that distorts the steady-state conditions is the asynchrony in the modulation carriers that grow with the packet loss interval since the synchronization of carriers is interrupted. The carrier asynchrony results in harmonic distortion in the ac-side variables, submodule-capacitor-voltage unbalance, and ripple in the circulating current [12], [34]. Thus, the carrier asynchrony makes the proposed autonomous control unsuitable for unlimited operation time even if all the other circuit parameters stay the same throughout the loss interval. Then, the autonomous control mode can be sustained in a submodule until its local measurements, i.e., the submodule capacitor voltage and arm current, hit the predefined limits, which can be set according

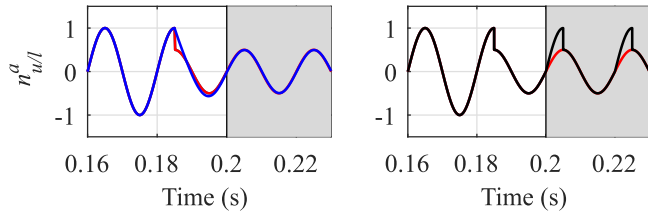


**Fig. 4.** Resonant controller (left, blue) versus moving table (right, black) for the autonomous insertion index generation. At 0.185 s, the ideal insertion index (red) amplitude decreases from 1 to 0.5. Packet loss is decided at 0.2 s.

to the component ratings. The period that the measurements hit the limits depends on the changes in the circuit variables, if any, and the dynamics that affect the carrier asynchrony [34]. A more vigilant alternative for the autonomous control interval would be limiting it to a few fundamental periods, e.g., two, and also checking the local measurements. The ultimate decision should be made by the operator considering the related risk assessment. If the local measurements hit the limits or if the communication is still not recovered after the predefined interval, it would be more suitable for a submodule to stop the autonomous operation and switch to another operation mode which, possibly, is safety-oriented rather than performance-oriented. This article leaves a suitable scenario to implement in such extreme error intervals as future work. The authors hypothesize that the required work can be founded on the proposed autonomous insertion index generation mode. Moreover, the proposed control is not an alternative to the redundancy submodules, which are switched in to replace long-term faulty submodules provided that the redundancy submodules have a functioning wireless communication link [35].

An alternative to the proposed autonomous controllers would be recording the last fundamental period of indices in the submodule controllers in a “moving table” and using the recorded data when a packet loss occurs. This method can work in case the insertion indices vary in a steady-state fashion. However, if there is any change in the amplitude or phase of the received index in the last period before the packet loss, the table contents cannot be updated fully, and some obsolete indices have to be repeated in the autonomous mode. On the other hand, the resonant controllers can adapt to this change with a suitably set  $K_h$ . Fig. 4 illustrates such a case when the packet loss is decided shortly after an amplitude change in the insertion index. The resonant controller output (left, blue) adapts to the change, and it follows the ideal index (red) in the packet loss interval (0.2 s onward), while the moving table (right, black) repeats the last period with obsolete table elements.

#### IV. CASE STUDY AND EXPERIMENTAL VERIFICATION

##### A. Experimental Setup

The proposed autonomous submodule control is implemented on a single-phase laboratory-scale MMC consisting of half-bridge submodules and connected to a resistive load. The experimental setup is shown in Fig. 5. The MMC central and submodule controller hardware, wireless transceivers, the connections

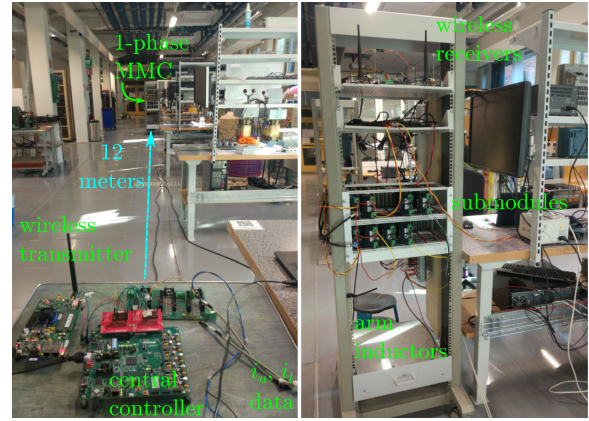


**Fig. 5.** Experimental setup: The central controller and its wireless transmitter and 1-phase MMC on the left, and wireless receivers on the right.

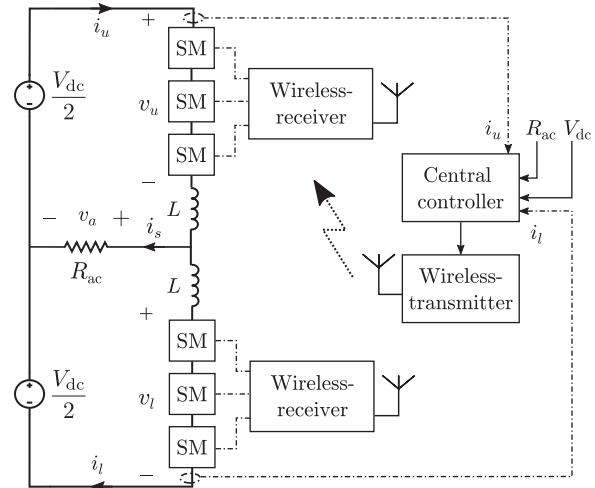


**Fig. 6.** Circuit diagram of the wirelessly controlled single-phase MMC experimental setup.

between those, and the employed wireless communication parameters are the same as in [13]. The central controller and the submodules are 12 m apart in the power electronics laboratory. The transceivers are in the line of sight. The circuit diagram of the setup is shown in Fig. 6.  $v_u$  and  $v_l$  are the inserted upper arm and lower arm voltages, respectively.  $v_a$  is the voltage across the load resistor.  $i_l$  and  $i_s$  are the lower arm and ac-side currents, respectively. The parameters of the MMC are given in Table I.

PR controllers regulate the ac-side and circulating currents as described in the preceding section. The ac-side current reference is defined in its controller as

$$i_s^* = \hat{i}_s^* \sin(\omega_1 t + \phi) = \frac{V_{dc}}{2} m_a \frac{1}{R_{ac}} \sin(\omega_1 t + \phi) \quad (12)$$

where  $\hat{i}_s^*$  is the peak value of  $i_s^*$  and  $m_a$  is the amplitude modulation index.  $\hat{i}_s^*$  is adjusted by changing  $m_a$  while keeping  $R_{ac}$  constant, as in Table I. Phase-shifted carrier-based modulation and individual submodule-capacitor-voltage control are employed in the submodules. The controller parameters are given in Table II. The parameters are chosen according to the controller design



TABLE I  
MMC PARAMETERS

	Symbol	Value
Fundamental frequency	$\omega_1$	$2\pi 50$ rad/s
Modulation carrier frequency	$f_c$	833 Hz
Submodules per arm	$N$	3
Offset between upper and lower arm carriers	$\beta^\dagger$	0 rad
Frequency tolerance of FPGA clocks	$\Delta f/f_{osc}$	50 ppm
Dc-side voltage	$V_{dc}$	100 V
Ac-side resistance	$R_{ac}$	10 $\Omega$
Arm parasitic resistance	$R$	0.3 $\Omega$
Arm inductance	$L$	3 mH
Submodule capacitance	$C_{sm}$	2.7 mF

$\dagger$  The value of  $\beta$  with odd  $N$  results in having the first group of switching harmonics around  $2Nf_c$ .

TABLE II  
CONTROLLER PARAMETERS

	Symbol	Value
Sampling frequency	$\omega_s$	$2\pi 10$ krad/s
Ac-side-current controller closed-loop-system bandwidth	$\alpha_c$	$\frac{\omega_s}{10(5+1)}$ [rad/s]
Ac-side-current controller proportional gain	$K_p$	$\alpha_c L/2$ [ $\Omega$ ]
Ac-side-current resonant controller bandwidth	$\alpha_1$	$\alpha_c/10$ [rad/s]
Ac-side-current controller resonant gain	$K_1$	$\alpha_1 \alpha_c L$ [ $\Omega/s$ ]
Circulating-current controller virtual resistance	$R_a$	$\alpha_c L/2$ [ $\Omega$ ]
Circulating-current resonant controller bandwidth	$\alpha_2$	50 rad/s
Circulating-current controller resonant gain	$K_2$	100 $\Omega/s$
Open-loop voltage controller band-pass filter bandwidth	$\alpha_f$	31 rad/s
Total time delay from the central controller to the submodules [13]	$T_d$	242 $\mu s$

suggestions in [32]; the processes are not repeated for brevity. The ac-side and circulating current controller block diagrams and their parameters are the same as in [13, Fig. 6] and [13, Table II]. The reader is referred to [13, Sec. IV.D] to get an insight into the total time delay,  $T_d$ , components and to investigate the closed-loop system stability. The ac-side and circulating current closed-loop systems are stable with  $71^\circ$  and  $49^\circ$  phase margins.

### B. Packet Loss Characteristics of the Experimental Setup

The packet loss characteristics of the experimental setup are observed in ten measurements of 10-min operation intervals. The MMC is operated with  $\hat{i}_s^*$  equal to 4.75 A. The measurements are conducted in a stationary environment with no other equipment operating nearby, and the results are taken from one submodule. The losses highly depend on the spatial diversity of the wireless transmitter in the range of the communication signal wavelength. In a good placement of the transmitter, up to three consecutive packets are lost, while in a bad placement, it is up to 20 consecutive packets. Similarly, the packet loss rates change significantly. The mean values of the loss rates of ten measurements are  $7 \times 10^{-4}$  and  $9 \times 10^{-2}$  for the good and bad placement of the transmitter, respectively.

In industrial MMC stations, an enclosure around the control units while the chassis is connected to the earth is common to provide electromagnetic immunity from nearby interference

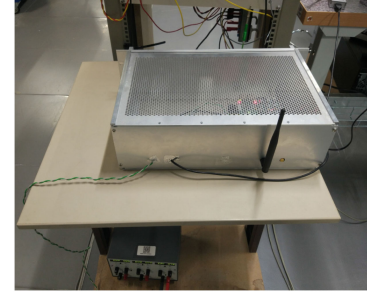


Fig. 7. Wireless receiver and submodule controller enclosed in an earthed aluminum box.

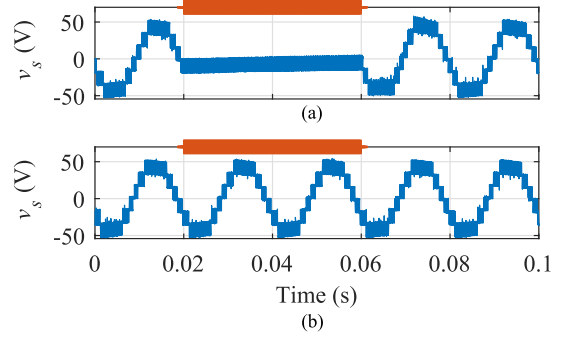


Fig. 8. AC-side voltage with (a) the existing and (b) the proposed control methods.

sources. Another set of measurements is carried out to investigate the feasibility of communication when the wireless antennas are put outside the enclosure. One submodule control unit with its wireless receiver is placed in an earthed aluminum enclosure while keeping the receiver antenna outside, as seen in Fig. 7. The packet losses are measured from the control unit during six consecutive 10-min intervals. The measurements are repeated when the enclosure lid is removed. The packet loss rates of the individual measurements are close to each other for the two campaigns, and the average loss rates are  $1.5 \times 10^{-3}$  and  $1.4 \times 10^{-3}$  for the campaigns with and without the enclosure lid, respectively. (The slight difference between the rates is considered because of the time variance of wireless communication.) The measurements reveal the possibility of keeping the antennas out of the enclosure.

### C. Results and Discussion

The proposed autonomous submodule control is benchmarked with the existing control in [13]. To see the performance of the proposed control clearly, the wireless transmission from the central controller is disabled for two cycles (40 ms). None of the submodules receives wireless data during this interval. In the proposed control, the fundamental and second harmonic resonant controllers are employed in  $G_o(s)$  in Fig. 3, with  $K_1$  as 1000 rad/s and  $K_2$  as 30 rad/s.  $T_{loss}$  is set to  $2.1 T_s$ .

The ac-side voltage, arm currents, circulating current, and one submodule capacitor voltage of the MMC are shown in Figs. 8–10. The packet loss interval is from 0.02 to 0.06 s, shown in the figures by a straight line on the top border. The submodules with the existing control method operate as



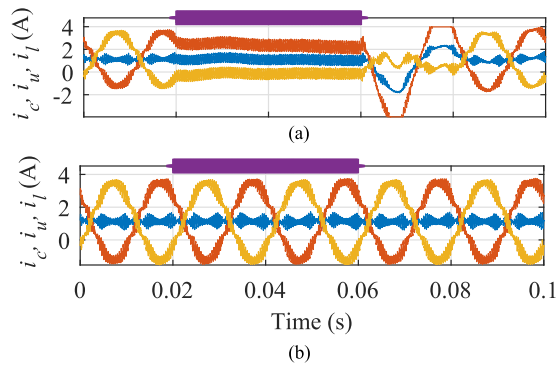


Fig. 9. Upper arm (orange), lower arm (yellow), and circulating current (blue) with (a) the existing and (b) the proposed control methods.

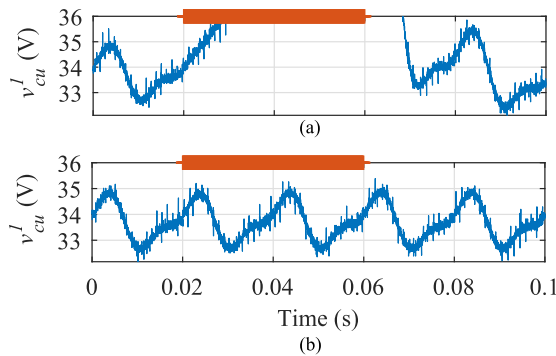


Fig. 10. Capacitor voltage of a submodule with (a) the existing and (b) the proposed control methods.

if a dc-to-dc converter resulting in a constant ac-side voltage, constant arm currents, and overcharged submodule capacitors. It can be deduced that if the load were active, overcurrents would have resulted. With the proposed control method, the submodules switch to the autonomous insertion index generation mode and continue modulation properly during the packet loss. The ac-side voltage, upper arm, lower arm, circulating currents, and submodule capacitor voltages follow their pattern before the packet loss.

The experimental results verify the functionality of the proposed autonomous submodule controller. It is considered that the functionality of the method is evident for shorter packet losses and when only one or some of the submodules experience losses instead of all. The method does not bring any drawback for the error-free interval while facilitating a smooth, uninterrupted operation throughout the losses. However, it should be remembered that the modulation continues with the dynamics before the loss train, and any change by the central controller would not be implemented until the communication is recovered. To illustrate this phenomenon, an experiment is conducted in which  $R_{ac}$  is decreased to  $2/3$  of its value in Table I during the packet loss interval and  $\hat{i}_s^*$  is kept at 5 A. The ac-side current, arm currents, circulating current, and one submodule capacitor voltage of the MMC are shown in Fig. 11. The load change happens around the first zero-crossing of the ac-side current after the loss train starts. As  $R_{ac}$  decreases,  $\hat{i}_s$  increases to  $3/2$  of its reference. It decreases back to the reference only after the communication is recovered as the insertion index change by the

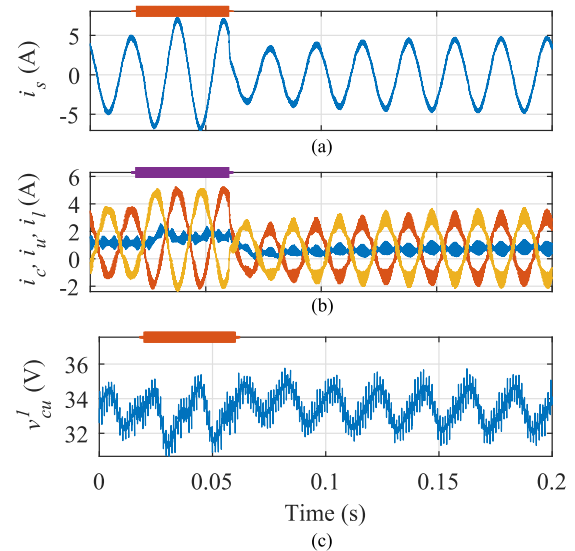


Fig. 11. (a) AC-side current, (b) upper arm (orange), lower arm (yellow), and circulating current (blue), and (c) capacitor voltage of a submodule with the proposed control method when the load changes during the packet loss interval.

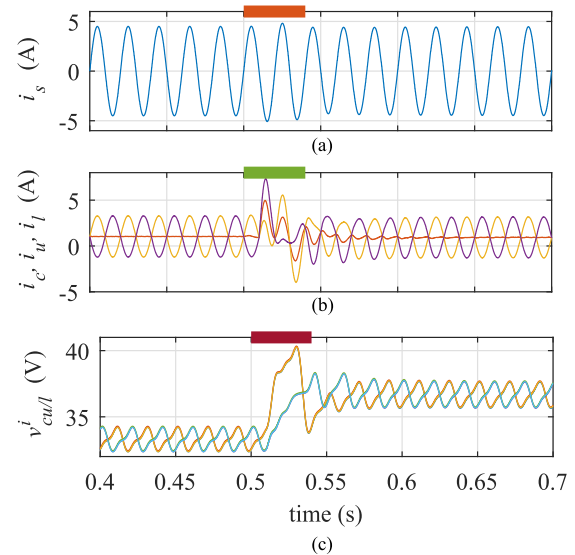


Fig. 12. (a) AC-side current, (b) upper arm (yellow), lower arm (purple), and circulating current (orange), and (c) submodule capacitor voltages with the proposed control method when the dc-side voltage changes during the packet loss interval.

central controller can be implemented then. As a further study, a simulation is performed in MATLAB/Simulink to investigate the dc-side voltage change during the communication loss. The simulation parameters are chosen the same as in the experiments.  $V_{dc}$  is increased to 1.1 times its value in Table I 10 ms after the start of the packet loss and  $\hat{i}_s^*$  is kept at 4.5 A. The ac-side current, arm currents, circulating current, and submodule capacitor voltages of the MMC are shown in Fig. 12. The response of the submodule controllers is similar to the case of load change. However, the dc-side voltage change has a higher impact on the arm currents and circulating current since there is a mismatch between the dc-side voltage and sum capacitor voltages when

the dc-side voltage increases. It is proposed that, as discussed in Section III-C, if an arm current increases above the safety limit, the related submodule controllers should switch to the safety-oriented control mode, which is left as future work.

## V. CONCLUSION

The wireless control of MMC submodules requires an advanced control system that can withstand long packet losses. The previously proposed wireless control method was based on transmitting the insertion indices wirelessly to the submodules from a central controller. This article advanced the proposed method by generating the indices autonomously in the submodules during the packet losses. The submodules generated their indices based on the previously received packets, continued modulation smoothly, and then returned to the closed-loop control when they received data from the central controller. The experimental results verified the functionality of the method. The proposal can be taken as a basis for further autonomy studies of the submodules that take submodule local variables into account, such as submodule capacitors charge/discharge and arm current passing through the submodules if current sensors are present. Moreover, the proposal can be used in wired distributed MMC control applications against the errors that wired networks can experience.

## ACKNOWLEDGMENT

The authors would like to thank Dr. Sebastian Schiessl for his contributions to the wireless network design.

## REFERENCES

- [1] S. Denetiere, S. Nguéfeu, H. Saad, and J. Mahseredjian, "Modeling of modular multilevel converters for the France-Spain link," in *Proc. Int. Conf. Power Syst. Transients*, 2013, pp. 1–7.
- [2] H.-J. Knaak, "Modular multilevel converters and HVDC/FACTS: A success story," in *Proc. 14th Eur. Conf. Power Electron. Appl.*, 2011, pp. 1–6.
- [3] Inelfe, "The electricity interconnection across the Biscay Gulf.," Accessed: Sep. 5, 2021. [Online]. Available: <https://www.inelfe.eu/en/projects/bay-biscay>
- [4] L. Brand *et al.*, "Testing and commissioning of VSC HVDC systems," *Cigre, Tech. Brochure* 697, Aug. 2017.
- [5] T. J. Stott and P. R. Couch, "Optical communications network for high voltage direct current power transmission," French Patent, WO2013178249A1, Dec. 5, 2013.
- [6] J. F. Allaire *et al.*, "Fire aspects of HVDC thyristor valves and valve halls," *Cigre, Tech. Brochure* 136, Feb. 1999.
- [7] M. A. Parker, L. Ran, and S. J. Finney, "Distributed control of a fault-tolerant modular multilevel inverter for direct-drive wind turbine grid interfacing," *IEEE Trans. Ind. Electron.*, vol. 60, no. 2, pp. 509–522, Feb. 2013.
- [8] C. L. Toh and L. E. Norum, "Implementation of high speed control network with fail-safe control and communication cable redundancy in modular multilevel converter," in *Proc. 15th Eur. Conf. Power Electron. Appl.*, 2013, pp. 1–10.
- [9] B. P. McGrath, D. G. Holmes, and W. Y. Kong, "A decentralized controller architecture for a cascaded H-bridge multilevel converter," *IEEE Trans. Ind. Electron.*, vol. 61, no. 3, pp. 1169–1178, Mar. 2014.
- [10] L. Mathe, P. D. Burlacu, and R. Teodorescu, "Control of a modular multilevel converter with reduced internal data exchange," *IEEE Trans. Ind. Informat.*, vol. 13, no. 1, pp. 248–257, Feb. 2017.
- [11] S. Yang, Y. Tang, and P. Wang, "Distributed control for a modular multilevel converter," *IEEE Trans. Power Electron.*, vol. 33, no. 7, pp. 5578–5591, Jul. 2018.
- [12] B. Ciftci, J. Gross, S. Norrga, L. Kildehøj, and H.-P. Nee, "A proposal for wireless control of submodules in modular multilevel converters," in *Proc. 20th Eur. Conf. Power Electron. Appl.*, 2018, pp. 1–10.
- [13] B. Ciftci, S. Schiessl, J. Gross, L. Harnefors, S. Norrga, and H.-P. Nee, "Wireless control of modular multilevel converter submodules," *IEEE Trans. Power Electron.*, vol. 36, no. 7, pp. 8439–8453, Jul. 2021.
- [14] M. Luvisotto, Z. Pang, and D. Dzung, "High-performance wireless networks for industrial control applications: New targets and feasibility," *Proc. IEEE*, vol. 107, no. 6, pp. 1074–1093, Jun. 2019.
- [15] S. Vitturi, C. Zunino, and T. Sauter, "Industrial communication systems and their future challenges: Next-generation Ethernet, IIoT, and 5G," *Proc. IEEE*, vol. 107, no. 6, pp. 944–961, Jun. 2019.
- [16] P. Dan Burlacu, L. Mathe, M. Rejas, H. Pereira, A. Sangwongwanich, and R. Teodorescu, "Implementation of fault tolerant control for modular multilevel converter using EtherCAT communication," in *Proc. IEEE Int. Conf. Ind. Technol.*, 2015, pp. 3064–3071.
- [17] S. Yang, H. Chen, P. Sun, H. Wang, F. Blaabjerg, and P. Wang, "Resilient operation of an MMC with communication interruption in a distributed control architecture," *IEEE Trans. Power Electron.*, vol. 36, no. 10, pp. 12057–12069, Oct. 2021.
- [18] D. N. Zmood and D. G. Holmes, "Stationary frame current regulation of PWM inverters with zero steady-state error," *IEEE Trans. Power Electron.*, vol. 18, no. 3, pp. 814–822, May 2003.
- [19] P. C. Tan, P. C. Loh, and D. G. Holmes, "High-performance harmonic extraction algorithm for a 25 kV traction power quality conditioner," *IEE Proc. Electric Power Appl.*, vol. 151, no. 5, pp. 505–512, Sep. 2004.
- [20] R. I. Bojoi, G. Griva, V. Bostan, M. Guerriero, F. Farina, and F. Profumo, "Current control strategy for power conditioners using sinusoidal signal integrators in synchronous reference frame," *IEEE Trans. Power Electron.*, vol. 20, no. 6, pp. 1402–1412, Nov. 2005.
- [21] R. Teodorescu, F. Blaabjerg, M. Liserre, and P. C. Loh, "Proportional-resonant controllers and filters for grid-connected voltage-source converters," *IEE Proc. Electric Power Appl.*, vol. 153, no. 5, pp. 750–762, Sep. 2006.
- [22] L. Harnefors, A. G. Yepes, A. Vidal, and J. Doval-Gandoy, "Passivity-based stabilization of resonant current controllers with consideration of time delay," *IEEE Trans. Power Electron.*, vol. 29, no. 12, pp. 6260–6263, Dec. 2014.
- [23] L. Ångquist, A. Antonopoulos, D. Siemaszko, K. Ilves, M. Vasiladiotis, and H.-P. Nee, "Open-loop control of modular multilevel converters using estimation of stored energy," *IEEE Trans. Ind. Appl.*, vol. 47, no. 6, pp. 2516–2524, Nov./Dec. 2011.
- [24] J. Zhang, T. Lu, W. Zhang, H. Shen, and Z. Yang, "Frequency-time domain characteristics of radiated electric fields in a multi-terminal MMC-HVDC station," *IEEE Access*, vol. 7, pp. 99937–99944, 2019.
- [25] W. Chen, L. Jia, L. Yu, and M. Li, "Measurement and analysis of electromagnetic disturbances in 500 kV DC converter station," in *Proc. China Int. Conf. Electricity Distrib.*, 2012, pp. 1–5.
- [26] A. Abdrabou and A. M. Gaouda, "Uninterrupted wireless data transfer for smart grids in the presence of high power transients," *IEEE Syst. J.*, vol. 9, no. 2, pp. 567–577, Jun. 2015.
- [27] C. Klünder and J. Luiken ter Haseborg, "Effects of high-power and transient disturbances on wireless communication systems operating inside the 2.4 GHz ISM band," in *Proc. IEEE Int. Symp. Electromagn. Compat.*, 2010, pp. 359–363.
- [28] A. Willig, K. Matheus, and A. Wolisz, "Wireless technology in industrial networks," *Proc. IEEE*, vol. 93, no. 6, pp. 1130–1151, Jun. 2005.
- [29] C. A. G. D. Silva and C. M. Pedroso, "MAC-layer packet loss models for Wi-Fi networks: A survey," *IEEE Access*, vol. 7, pp. 180512–180531, 2019.
- [30] S. Sahoo, T. Dragičević, and F. Blaabjerg, "Cyber security in control of grid-tied power electronic converters-challenges and vulnerabilities," *IEEE J. Emerg. Sel. Topics Power Electron.*, vol. 9, no. 5, pp. 5326–5340, Oct. 2021.
- [31] A. Willig, M. Kubisch, C. Hoene, and A. Wolisz, "Measurements of a wireless link in an industrial environment using an IEEE 802.11-compliant physical layer," *IEEE Trans. Ind. Electron.*, vol. 49, no. 6, pp. 1265–1282, Dec. 2002.
- [32] K. Sharifabadi, L. Harnefors, H.-P. Nee, S. Norrga, and R. Teodorescu, *Design Control and Application of Modular Multilevel Converters for HVDC Transmission Systems*. Chichester, U.K.: Wiley, 2016.
- [33] S. Golestan, M. Ramezani, J. M. Guerrero, F. D. Freijedo, and M. Monfared, "Moving average filter based phase-locked loops: Performance analysis and design guidelines," *IEEE Trans. Power Electron.*, vol. 29, no. 6, pp. 2750–2763, Jun. 2014.
- [34] H. Wang, S. Yang, H. Chen, X. Feng, and F. Blaabjerg, "Synchronization for an MMC distributed control system considering disturbances introduced by submodule asynchrony," *IEEE Trans. Power Electron.*, vol. 35, no. 12, pp. 12834–12845, Dec. 2020.

- [35] B. Li, Y. Zhang, R. Yang, R. Xu, D. Xu, and W. Wang, "Seamless transition control for modular multilevel converters when inserting a cold-reserve redundant submodule," *IEEE Trans. Power Electron.*, vol. 30, no. 8, pp. 4052–4057, Aug. 2015.



**Barış Çiftçi** (Student Member, IEEE) was born in Nazilli, Turkey, in 1987. He received the B.Sc. and M.Sc. degrees in electrical and electronics engineering from Middle East Technical University, Ankara, Turkey, in 2011 and 2014, respectively. He is currently working toward the Ph.D. degree in electrical engineering with the KTH Royal Institute of Technology, Stockholm, Sweden.

From 2011 to 2017, he was a Design Engineer and a Systems Engineer with Aselsan, Ankara, Turkey. His research focuses on wireless control of modular multilevel converter submodules.



**Lennart Harnefors** (Fellow, IEEE) received the M.Sc., Licentiate, and Ph.D. degrees in electrical engineering from the Royal Institute of Technology (KTH), Stockholm, Sweden, in 1993, 1995, and 1997, respectively, and the Docent (D.Sc.) degree in industrial automation from Lund University, Lund, Sweden, in 2000.

From 1994 to 2005, he was with Mälardalen University, Västerås, Sweden, and in 2001 as a Professor of Electrical Engineering. From 2001 to 2005, he was also a Part-Time Visiting Professor of Electrical Drives with the Chalmers University of Technology, Göteborg, Sweden. In 2005, he joined ABB, HVdc Product Group, Ludvika, Sweden, where, among other duties, he led the control development of the first generation of multilevel-converter HVDC Light. In 2012, he joined ABB, Corporate Research, Västerås, where he was a Senior Principal Scientist in 2013 and a Corporate Research Fellow in 2021. He is currently a Part-Time Adjunct Professor of Power Electronics with KTH. His research interests include control and dynamic analysis of power electronic systems, particularly grid-connected converters and ac drives.

Dr. Harnefors is the Editor of the *IEEE JOURNAL OF EMERGING AND SELECTED TOPICS IN POWER ELECTRONICS* and an Associate Editor for *IET Electric Power Applications*. He was the Recipient of the 2020 IEEE Modeling and Control Technical Achieved Award.



**Xiongfei Wang** (Senior Member, IEEE) received the B.S. degree from Yanshan University, Qinhuangdao, China, in 2006, the M.S. degree from Harbin Institute of Technology, Harbin, China, in 2008, both in electrical engineering, and the Ph.D. degree in energy technology from Aalborg University, Aalborg, Denmark, in 2013. From 2009 he has been with the Department of Energy Technology, Aalborg University, where he became an Assistant Professor in 2014, an Associate Professor in 2016, a Professor and

Leader of Electronic Power Grid (eGRID) Research Group in 2018. He has also been a Part-Time Professor at KTH Royal Institute of Technology, Stockholm, Sweden, from 2020. His current research interests include modeling and control of power electronic converters and systems, stability and power quality of power-electronics-dominated power systems, high-power converters.

Dr. Wang serves as a Member-at-Large of Administrative Committee for the IEEE Power Electronics Society (PELS) in 2020-2022, a Co-Editor-in-Chief for the *IEEE Transactions on Power Electronics Letters*, and as an Associate Editor for the *IEEE Journal of Emerging and Selected Topics in Power Electronics (JESTPE)*. He was selected into Aalborg University Strategic Talent Management Program in 2016. He has received six Prize Paper Awards in the IEEE Transactions and conferences, the 2018 Richard M. Bass Outstanding Young Power Electronics Engineer Award, the 2019 IEEE PELS Sustainable Energy Systems Technical Achievement Award, the 2020 IEEE Power & Energy Society Prize Paper Award, the 2020 JESTPE Star Associate Editor Award, and the Highly Cited Researcher in the Web of Science in 2019-2021.



**James Gross** (Senior Member, IEEE) received the Ph.D. degree in telecommunications engineering from TU Berlin, Berlin, Germany, in 2006.

From 2008 to 2012, he was an Assistant Professor and a Research Associate with the Center of Excellence on Ultra-High Speed Mobile Information and Communication (UMIC), RWTH Aachen University, Aachen, Germany. Since November 2012, he has been a Professor of machine-to-machine communications with the Electrical Engineering and Computer Science School, KTH Royal Institute of Technology, Stockholm, Sweden. From 2016 to 2019, he was the Director of the ACCESS Linnaeus Centre, KTH. He is currently an Associate Director of the newly formed KTH Digital Futures Research Center, and the Co-Director of the newly formed VINNOVA Competence Center on Trustworthy Edge Computing Systems and Applications (TECoSA). He is the Co-Founder of R3 Communications GmbH, a Berlin-based venture capital-backed company in the area of ultra-reliable low-latency wireless networking for industrial automation. He has authored more than 150 peer-reviewed papers in international journals and conferences. His research interests include mobile systems and networks, with a focus on critical machine-to-machine communications, edge computing, resource allocation, and performance evaluation.

Dr. James was the recipient of multiple awards, including the Best Paper Awards at ACM MSWiM 2015, IEEE WoWMoM 2009, and European Wireless 2009, and the ITG/KuVS Dissertation Award for his Ph.D. thesis in 2007.



**Staffan Norrga** (Member, IEEE) was born in Lidingö, Sweden, in 1968. He received the M.Sc. degree in applied physics from the Linköping Institute of Technology, Linköping, in 1993 and the Ph.D. degree in electrical engineering from the KTH Royal Institute of Technology, Stockholm, Sweden, in 2005.

Between 1994 and 2011, he was a Development Engineer with ABB, Västerås, Sweden, in various power-electronics-related areas such as railway traction systems and converters for HVdc power transmission systems. He is currently an Associate Professor in power electronics with KTH. He is the inventor or Co-inventor of more than ten granted patents and has authored or coauthored more than 100 scientific papers published at international conferences or journals. His research interests include power electronics and its applications in power grids, renewables, and electric vehicles.



**Hans-Peter Nee** (Fellow, IEEE) was born in Västerås, Sweden, in 1963. He received the M.Sc., Licentiate, and Ph.D. degrees in electrical engineering from the KTH Royal Institute of Technology, Stockholm, Sweden, in 1987, 1992, and 1996, respectively.

Since 1999, he has been a Professor of Power Electronics with the Department of Electrical Engineering, KTH Royal Institute of Technology. His research interests include power electronic converters, semiconductor components, and control aspects of utility applications, such as FACTS and high-voltage direct-current transmission, and variable-speed drives.

Dr. Nee was a Member of the Board of the IEEE Sweden Section for many years and was the Chair of the Board from 2002 to 2003. He is also a Member of the European Power Electronics and Drives Association and is involved with its Executive Council and International Steering Committee.